

Published in final edited form as:

Vascul Pharmacol. 2017 February ; 89: 39–48. doi:10.1016/j.vph.2017.01.002.

GPR55 agonist lysophosphatidylinositol and lysophosphatidylcholine inhibit endothelial cell hyperpolarization via GPR-independent suppression of Na⁺-Ca²⁺ exchanger and endoplasmic reticulum Ca²⁺ refilling

Alexander I. Bondarenko^{a,b,*}, Fabrizio Montecucco^{c,d}, Olga Panasiuk^a, Vadim Sagach^a, Nataliya Sidoryak^e, Karim J. Brandt^f, and François Mach^f

^aCirculatory Physiology Department, Bogomoletz Institute of Physiology NAS of Ukraine, Bogomoletz Str.4, 01024 Kiev, Ukraine ^bMedical University of Graz, Institute of Molecular Biology and Biochemistry, Graz 8010, Austria ^cFirst Clinic of Internal Medicine, Department of Internal Medicine, University of Genoa, 6 viale Benedetto XV, 16132 Genoa, Italy ^dIRCCS AOU San Martino - IST Istituto Nazionale per la Ricerca sul Cancro, Largo Benzi 10, 16132 Genoa, Italy ^eDepartment of Physiology of Human and Animals, Melitopol State Pedagogical University, Ukraine ^fDivision of Cardiology, Foundation for Medical Researches, Department of Internal Medicine, University of Geneva, Av. de la Roseraie 64, CH-1211 Geneva 4, Switzerland

Abstract

Lysophosphatidylinositol (LPI) and lysophosphatidylcholine (LPC) are lipid signaling molecules that induce endothelium-dependent vasodilation. In addition, LPC suppresses acetylcholine (Ach)-induced responses. We aimed to determine the influence of LPC and LPI on hyperpolarizing responses in vitro and in situ endothelial cells (EC) and identify the underlying mechanisms. Using patch-clamp method, we show that LPI and LPC inhibit EC hyperpolarization to histamine and suppress Na⁺/Ca²⁺ exchanged (NCX) currents in a concentration-dependent manner. The inhibition is non-mode-specific and unaffected by intracellular GDPβS infusion and tempol, a superoxide dismutase mimetic. In excised mouse aorta, LPI strongly inhibits the sustained and the peak endothelial hyperpolarization induced by Ach, but not by SKA-31, an opener of Ca²⁺-dependent K⁺ channels of intermediate and small conductance. The hyperpolarizing responses to consecutive histamine applications are strongly reduced by NCX inhibition. In a Ca²⁺-re-addition protocol, bepridil, a NCX inhibitor, and KB-R7943, a blocker of reversed NCX, inhibit the hyperpolarizing responses to Ca²⁺-re-addition following Ca²⁺ stores depletion. These findings indicate that LPC and LPI inhibit endothelial hyperpolarization to Ach and histamine independently of G-protein coupled receptors and superoxide anions. Reversed NCX is critical for ER Ca²⁺ refilling in EC. The inhibition of NCX by LPI and LPC underlies diminished

*Corresponding author at: Circulatory Physiology Department, Bogomoletz Institute of Physiology NAS of Ukraine, Kiev 01024, Ukraine. abond01@biph.kiev.ua (A.I. Bondarenko).

Conflict of interest

All authors declare no conflict of interest.

endothelium-dependent responses and endothelial dysfunction accompanied by increased levels of these lipids in the blood.

Keywords

Lysophosphatidylinositol; Lysophosphatidylcholine; Endothelial cells; Hyperpolarization; Na⁺-Ca²⁺ exchanger

1 Introduction

Long-chain lysophospholipids (LPL) are recognized as potent signaling molecules that regulate a variety of biological processes. In vascular physiology, among distinct LPL, lysophosphatidylinositol (LPI) and lysophosphatidylcholine (LPC) have attracted considerable attention due to their vasoactive properties, complex pharmacology and pathophysiological relevance [1]. Elevated levels of LPC, a major ingredient of oxidized low-density lipoproteins (LDL), are closely associated with the development of atherosclerosis [2,3], an early manifestation of which is endothelial dysfunction [4]. In animal and human studies, the atherosclerotic process is frequently characterized by an impaired acetylcholine (Ach)-induced endothelium-dependent vasodilation and reduced bioavailability of endothelium-derived nitric oxide (NO) [4–6]. LPC and LPI were shown to induce atherogenic activities, including the induction of vascular cell adhesion molecules (VCAM-1) and intracellular adhesion molecules (ICAM-1) [1,7,8]. In addition, LPC and LPI stimulate migration of smooth muscle cells [8], a crucial process in the pathogenesis of atherosclerosis.

The impact of LPC and LPI on vascular function remains controversial. On the one hand, several animal and clinical studies have demonstrated that LPC produces endothelium-dependent nitric oxide (NO)-mediated relaxation [9–11] accompanied by an increase of intracellular Ca²⁺ concentration in endothelial cells (EC) [12–15]. In the human umbilical vein EC (HUVECs) model, it was proposed that LPC-stimulated Ca²⁺ entry leads to activation of BK_{Ca} channels coupled to an increase of ROS production [16]. On the other hand, it is well documented that in a vast number of vascular beds LPC actually inhibits or completely abrogates endothelium-dependent relaxation induced by Ach and bradykinin [17–22]. This effect is accompanied by strong inhibition of Ca²⁺ mobilization in EC [19] and almost full suppression of smooth muscle cell hyperpolarization to Ach [23].

Different mechanisms have been proposed to underpin the effect of LPC on endothelium-dependent relaxation, such as generation of procontracting prostanoids [24] and superoxide anions [22,25], a decreased release of Ach-stimulated NO, endothelium-derived hyperpolarizing factor (EDHF), or both of the latter two mechanisms [25–28]. However, none of the studies addressed the underlying alterations in specific ion transport systems in EC caused by LPC. Collectively, the mechanisms underlying both the promotion and inhibition of endothelium-dependent relaxation by LPC are still not fully unveiled.

Similar paradoxical observations have been reported in studies addressing the impact of LPI, a GPR55 agonist [29], on vascular contractility. In precontracted rat mesentery, LPI

produces endothelium-dependent relaxation accompanied by elevation of intracellular Ca^{2+} in primary EC [30] and EC line EA.hy926 [31]. However, in the same vascular bed, LPI was shown to strongly suppress endothelium-dependent hyperpolarization to Ach [23]. Irrespective of the nature of endothelium-dependent relaxation (NO or EDHF), the ability of EC to generate normal hyperpolarizing responses is of utmost importance and prerequisite for proper EC function [32–34]. While early reports point for engagement of Na^+ - Ca^{2+} exchanger (NCX) to Ca^{2+} extrusion from EC following administration of IP_3 -generating agents [35,36], more recent data indicate that NCX operates in a reversed mode, contributing to membrane hyperpolarization during stimulation with Ach [37] and histamine [38,39] and controlling angiogenesis [40]. Accordingly, in the present study we addressed the impact of the LPC and LPI action on endothelial hyperpolarization induced by Ach and histamine and NCX currents. We show that both LPI and LPC strongly inhibit the hyperpolarizing responses via direct G-protein coupled receptor (GPCR)-independent inhibition of Ca^{2+} influx via reversed NCX. In contrast, in resting cells, LPC produces EC hyperpolarization via direct stimulation of BK_{Ca} channels independently of GPCR and Ca^{2+} entry. In addition, we extend our previous finding that identified NCX as Ca^{2+} influx pathway into the endothelium during stimulation with Ach [37] by showing that reversed NCX is crucial for endoplasmic reticulum Ca^{2+} refilling in EC.

2 Methods

2.1 Animals and tissue preparation

Experiments were performed on C57Bl/6 mice of both sexes aged 12–16 weeks. Mice were sacrificed by cervical dislocation. Experiments were carried out in accordance with the U.K. Animals (Scientific Procedures) Act 1986 and EU Directive 2010/63/EU for animal experiments. All protocols employed in this study were approved by the Institutional Animal Ethics Committee, Bogomoletz Institute of Physiology. Thoracic aorta was excised, placed into physiological saline, cleaned and cut into segments of 2–3 mm under stereo microscope. One of the segments was cut open and pinned endothelial face up to the bottom of a recording chamber. Pharmacological agents were applied to the preparation by bath perfusion. Experiments were conducted at room temperature.

2.2 Cell culture

EA.hy926 cells (human umbilical vein-derived EC line, passages 30 and 85) [41] were grown in DMEM containing 10% fetal bovine serum, 1% penicillin/streptomycin and 1% HAT (5 mM hypoxanthin, 20 μM aminopterin, 0.8 mM thymidine) at 37 °C in 5% CO_2 atmosphere. They were plated on glass coverslips about 48 h before experiments.

2.3 Electrophysiological recordings

Membrane potential from the endothelium of excised mouse aorta was recorded using the nystatin-perforated patch-clamp technique, essentially as described previously [37]. In EA.hy926 cells, membrane potential was recorded using nystatin-perforated patch-clamp technique from electrically coupled cells. For membrane potential recordings, the standard bath solution contained (in mM): 140 NaCl, 5 KCl, 1.2 MgCl_2 , 10 HEPES, 10 glucose, 2.4 CaCl_2 . Patch pipettes were filled with a solution containing (in mM): 145 KCl; 0.3 EGTA;

10 HEPES (pH adjusted to 7.2 using KOH). The resistance of the pipettes was 3–5 M Ω . Whole-cell I_{NCX} was recorded using conventional whole cell patch-clamp technique. For recordings of both reversed and forward modes of the exchanger using voltage ramps, the bath solution contained (in mM): 140 NaCl, 5 TEACl, 2.4 CaCl₂, 1.2 MgCl₂, 10 HEPES, 10 glucose and the pipette solution contained (in mM): 110 Cs-methanesulfonate, 10 NaCl, 20 TEACl, 2 MgATP, 10 HEPES, 5 EGTA. Free Ca²⁺ concentration was set to 100 nM by adding 1.93 mM CaCl₂ calculated by the program CaBuf developed by G. Droogmans, Leuven, Belgium. Voltage ramps of 1 s duration from –100 mV to +90 mV were delivered every 5 s from the holding potential of –40 mV.

Single-channel BK_{Ca} activities were recorded from inside-out patches excised from EA.hy926 cells. The pipettes were filled with (in mM) 130 KCl, 10 HEPES, 1 MgCl₂, 5 EGTA, with adjusted free Ca²⁺ to 10 μ M by adding 4.931 mM CaCl₂ and pH 7.2 by adding KOH. After gigaseal formation, the bath solution was switched to the high K⁺ solution of the following composition: (in mM): 140 KCl, 10 HEPES, 1 MgCl₂, 5 EGTA and a desired free Ca²⁺ concentration adjusted by adding different amounts of CaCl₂ calculated by the program CaBuf. pH was adjusted to 7.1 by adding KOH.

2.4 Materials

LPC16:0 (1-palmitoyl-2-hydroxy-*sn*-glycero-3-phosphocholine) was purchased from Avanti Polar Lipids, LPI from Sigma Aldrich, paxilline and SKA-31 were purchased from Alomone Labs, KB-R7943 was purchased from TCI Chemicals.

2.5 Statistical analysis

Experimental data are expressed as mean \pm SEM. Student's *t*-test (paired or unpaired where appropriate) was used to compare results, with *p* < 0.05 taken as the level of significance. In experiments on EA.hy926 cells, *n* indicates the number of cells. In experiments presented herein, we used around 20 passages of this immortalized EC line. In experiments on intact EC from excised mice aorta, *n* indicates the number of animals.

3 Results

3.1 LPI and LPC16:0 reversibly inhibit EC hyperpolarization to histamine

In EA.hy926 cells, we first tested the sensitivity of the sustained hyperpolarization triggered by 100 μ M histamine to LPI and LPC16:0. When 10 μ M LPI was administered during the plateau phase of the hyperpolarization (27.8 ± 2.2 mV, *n* = 5), it was strongly inhibited and the response reversed to a depolarization with the mean amplitude of 2.6 ± 3.4 mV, *n* = 5 (Fig. 1A and B). The hyperpolarization was restored upon LPI wash-out. Similar to LPI, LPC16:0 (10 μ M) administered during the plateau phase of the hyperpolarization strongly inhibited the hyperpolarizing response within 3 min (Fig. 1C and D). The hyperpolarization did not recover in the continued presence of LPC16:0 and histamine but was reversed upon LPC wash-out. These results indicate that both LPI and LPC16:0 act as powerful inhibitors of EC hyperpolarization to histamine and are compatible with the previous studies showing suppression of Ca²⁺ transients [19] and endothelium-dependent hyperpolarization [23] to Ach by LPC16:0 and LPI.

3.2 LPC16:0-induced membrane hyperpolarization is due to direct activation of BK_{Ca} channels

To rule out the possibility that the inhibitory effect of LPC16:0 on endothelial hyperpolarization triggered by histamine is simply accounted by a strong depolarizing effect, we next examined the effects of LPC16:0 on the membrane potential of unstimulated EC. Administration of 3 μM LPC16:0 induced membrane hyperpolarization from the resting membrane potential -29.3 ± 2.4 mV to -40.6 ± 4.5 mV ($n = 9$, Fig. 2A). In voltage-clamp mode, LPC16:0 activated the outwardly rectifying current that was sensitive to paxilline, a BK_{Ca} inhibitor (Fig. 2B), indicating that the current activated by LPC16:0 is a BK_{Ca} current.

To explore whether the development of BK_{Ca} current by LPC16:0 requires changes in cytosolic Ca²⁺ concentration, single channel BK_{Ca} activity was recorded in inside-out patches under fixed Ca²⁺ concentration. In the presence of 0.3 μM Ca²⁺ in the bath, LPC16:0 administered to the inner surface of the patch stimulated the BK_{Ca} single channel activity. The degree of stimulation was similar within the voltage range from 20 to 70 mV (Fig. 3A and B), indicating that the stimulation occurred in a voltage-independent manner. When holding the voltage at 40 mV and Ca²⁺ fixed at 0.3 μM , the NPo values increased from 0.017 ± 0.001 to 0.028 ± 0.001 ($n = 9$) upon addition of 3 μM LPC16:0 (Fig. 3C).

3.3 LPI and LPC16:0 suppress both forward and reversed modes of NCX current independently of GPCR and superoxide anions

As reversed NCX contributes to the sustained endothelial hyperpolarization to Ach due to direct electrogenic effect and indirectly, via stimulation of K_{Ca} channels following Ca²⁺ inflow [37], we next explored whether the inhibitory effect of LPI and LPC16:0 on the hyperpolarization is attributed to inhibition of NCX. When potassium conductance was suppressed by cell dialysis with the Cs⁺-based solution containing low Ca²⁺ (100 nM) concentration and 10 mM Na⁺, voltage ramps from -100 to 85 mV produced an outwardly rectifying current with the reversal potential close to that calculated for NCX under our experimental conditions (-55 mV). This current was potentiated by histamine and further enhanced by a switch to a Na⁺-free solution (Fig. 4A and B), a maneuver widely used to trigger Ca²⁺ inflow via NCX. These observations, as well as sensitivity of the current to bepridil, a NCX inhibitor [42] (see below and [38]), are consistent with the increased activity of reversed NCX under these experimental conditions. Subsequent administration of LPI (1–10 μM) in Na⁺-free solution suppressed the currents in a concentration-dependent manner (Fig. 4A–C). The current was further inhibited by 100 μM bepridil (Fig. 4A and B). Due to increased risk of micelle formation at LPI concentration higher than 10 μM [43], higher concentrations of LPI have not been tested and, therefore, IC₅₀ was not possible to determine.

To rule out plausible role of store-operated Ca²⁺ entry (SOCE) activated following partial depletion of Ca²⁺ stores by histamine in the inhibitory effect of LPI, NCX-driven Ca²⁺ inflow was pre-stimulated by reduction of bath Na⁺ concentration (20 mM) only, without prior exposure with histamine. This procedure resulted in potentiation of outward current which was strongly suppressed by further administration of LPI (Fig. 4D).

We also examined the LPI effect on basal NCX currents, i.e. without prior exposure to histamine and a low Na⁺ solution. Under these conditions, LPI inhibited both outward (reversed mode) and inward current (forward mode) at positive and negative potentials, respectively, indicating that the effect of LPI on NCX is non-mode specific. LPI suppressed I_{NCX} when the pipette solution was supplemented with GDPβS (0.5 μM), a G-protein inhibitor (Fig. 4E and F), indicating that GPCR are not involved in the inhibitory effect.

Superoxide anions were shown to mediate the inhibitory effect of some LPCs on endothelium-dependent relaxation [22,25]. To investigate the role of superoxide in the observed effect of LPI, we next examined the influence of superoxide dismutase mimetic tempol on the effect of LPI on NCX current. Pre-incubation with tempol (10 μM) failed to prevent the inhibition of NCX current by 3 μM LPI (Fig. 4G). In the presence of 10 μM tempol, 3 μM LPI inhibited I_{NCX} in the forward (at -95 mV) and reversed (at 85 mV) modes to 29.8 ± 1.2% and 35.4 ± 3.8 (n = 4), respectively, of the initial values. The degrees of inhibition of both NCX modes were not significantly different (p = 0.12). No statistical difference was also detected in the degrees of I_{NCX} inhibition by 3 μM LPI in the absence and presence of tempol (n = 4, p > 0.1, Fig. 4H).

Next, we explored the effect of LPC16:0 on I_{NCX}. When reversed NCX was fostered by exposure of cells to histamine and Na⁺-free solution, administration of 3 μM LPC16:0 resulted in a gradual time-dependent suppression of the current to 46.8 ± 9.7% (n = 6) measured at 85 mV of the original amplitude (Fig. 5A, B and E). An increase in LPC16:0 concentration to 10 μM accelerated the time course of inhibition and further suppressed the current (Fig. 5C and D).

3.4 LPI suppresses endothelial hyperpolarization to Ach, but not to SKA-31, in excised mouse aorta

We next examined whether LPI modifies EC hyperpolarization to Ach in vascular tissue. In excised mice aorta, Ach (2 μM) produces a sustained EC hyperpolarization which was reversibly inhibited by LPI (3 μM) applied during the plateau phase (Fig. 6A). The effect of 10 μM LPI, however, was poorly reversible, likely because of accumulation of LPI in the tissue, and Ach failed to produce the hyperpolarizing responses shortly following LPI wash-out (Fig. 6B). In contrast, the hyperpolarization to SKA-31, an opener of Ca²⁺-dependent K⁺ channels of intermediate (IK_{Ca}) and small (SK_{Ca}) conductance, was unaffected either by pre-exposure to 10 μM LPI (Fig. 6B) or LPI administration during the hyperpolarization to SKA-31 (Fig. 6C).

3.5 Reversed mode of NCX is essential for endoplasmic reticulum (ER) Ca²⁺ refilling

Ca²⁺ release from intracellular stores accompanied by stimulation of IK_{Ca} channels underlies the initial transient endothelial hyperpolarization to Ach, while the sustained component requires Ca²⁺ entry [32, 44]. Considering the stimulatory effect of LPI on IK_{Ca} [43] and BK_{Ca} activity at low and moderate level of cytosolic Ca²⁺ [45], we can suggest that the failure of the endothelium to produce normal hyperpolarizing responses to Ach shortly following LPI wash-out may indicate that LPI inhibits Ca²⁺ refilling in the ER rather than IK_{Ca} channels. Accordingly, we next addressed the role of NCX in ER Ca²⁺ refilling.

Typical changes in membrane potential evoked by Ca^{2+} re-addition protocol are depicted in Fig. 7A. As expected, re-introduction of Ca^{2+} following wash out-of histamine in Ca^{2+} -free solution elicited a sustained hyperpolarization with the amplitude comparable with that evoked by histamine. In the presence of bepridil, the sustained hyperpolarization evoked by Ca^{2+} re-introduction was largely depressed (Fig. 7B). The hyperpolarization was restored following removal of bepridil. To further explore the impact of NCX on ER Ca^{2+} refilling, we also employed the protocol consisting of consecutive administrations of histamine in the continued presence of bepridil. Under these conditions, the cells failed to reproduce the hyperpolarizing responses (Fig. 7C).

Similar to bepridil, KB-R7943 (20 μM), a reversed mode NCX inhibitor, suppressed the hyperpolarization caused by Ca^{2+} -re-addition (Fig. 7D). Subsequent histamine administration in a Ca^{2+} -free solution followed by Ca^{2+} re-introduction in the continued presence of KB-R7943 produced weak changes in membrane potential. Altogether these results indicate that NCX operation in reversed mode is required for ER Ca^{2+} refilling during stimulation with Ach and histamine.

3.6 Buffering of intracellular Ca^{2+} uncovers Na^{+} -dependent membrane depolarization in response to histamine

The reversal of NCX during cell hyperpolarization requires a pronounced increase in $[\text{Na}^{+}]_i$. To further clarify the mechanism of NCX reversal, we used BAPTA-AM to chelate cytosolic Ca^{2+} in unstimulated cells and buffer an increase in cytosolic Ca^{2+} during cell stimulation with histamine. We expected that, according to NCX energetics, intracellular Ca^{2+} buffering would facilitate the reversed mode of NCX. Patch-clamping from electrically coupled cells minimized the impact of residual Ca^{2+} ions contained in the pipette solution on the level of cytosolic Ca^{2+}

EA.hy926 cells were loaded with 20 μM BAPTA-AM for 20 min at 37°C. In BAPTA-AM-pre-treated cells, the resting membrane potential appeared to be significantly ($p < 0.05$) more negative (-51.1 ± 1.9 , $n = 13$) than that observed in untreated cells (-34.6 ± 2.7 , $n = 11$, Fig. 8A). Cell superfusion with a Ca^{2+} -free solution induced cell depolarization by 17.2 ± 2.1 mV ($n = 4$, Fig. 8B). Bepridil (100 μM , Fig. 8C) and KB-R7943 (20 μM , Fig. 8D) elicited cell depolarization under these conditions. Taken together, these observations indicate that an increased Ca^{2+} entry mediated by electrogenic NCX contributes to the hyperpolarized resting membrane potential under conditions of cytoplasmic Ca^{2+} buffering. Administration of 100 μM histamine to BAPTA-AM pre-treated cells induced a strong depolarization with the mean amplitude of 45.6 ± 4.5 mV ($n = 12$) (Fig. 8E, F). Under these experimental conditions, chelation of extracellular Ca^{2+} with 1 mM EGTA failed to terminate the depolarization (Fig. 8G,H). The depolarization, however, was reversibly eliminated by substitution of extracellular Na^{+} with NMDG (Fig. 8G,H), indicating that stimulation of endothelial cells with histamine induces a massive Na^{+} influx. In addition, histamine applied in a Ca^{2+} free solution shortly after Ca^{2+} removal evoked a more sustained depolarization with a long decay as compared with that observed in a Ca^{2+} – containing solution (Fig. 8, E, G,H),

4 Discussion

Previous studies point for a close association between a decreased endothelium-dependent relaxation and an elevated content of oxidized LDL [4,46–48]. We demonstrate here that LPI and LPC strongly suppress the hyperpolarization of cultured EC stimulated with histamine. The inhibition was reversible following washing out of the compounds. This observation and the continued stability of patches in the presence of LPC16:0 and LPI indicates that these LPL at concentrations up to 10 μM suppress endothelium-dependent relaxation not through EC damage, but via functional modulation of specific ion-transporting systems.

We show that in EC, LPI and LPC effectively suppress outwardly rectifying currents pre-simulated by removal or lowering of external Na^+ , a maneuver commonly employed to activate the reverse NCX. These currents were previously shown to be highly sensitive to bepridil and KB-R7943, two structurally different NCX inhibitors [38,39]. The current inhibition by LPI and LPC16:0 occurred over the same concentration range as the inhibition of the hyperpolarizing responses to histamine. Noteworthy, at 10 μM LPI and LPC16:0 strongly inhibited NCX currents even when intracellular Ca^{2+} stores had not been depleted by prior histamine exposure. Thus, we conclude that LPI and LPC16:0 inhibit EC hyperpolarization through suppression of NCX function rather than SOCE inhibition. In addition, the ability of LPI and LPC to inhibit basal I_{NCX} both at positive and negative voltages indicates that the inhibitory effect is non-mode-specific.

Because cell infusion with GDP β S failed to prevent the inhibitory action of LPI, our results further indicate that the inhibitory action of LPI on I_{NCX} is not mediated by GPCR. Apart from NCX, EC hyperpolarization to Ach is partially mediated by $\alpha 1$, but not $\alpha 2$ or $\alpha 3$ isoforms of Na^+/K^+ -ATPase [49]. In EC, LPI was recently shown to suppress Na^+/K^+ -ATPase [31] and, hence, this effect may additionally contribute to the inhibition of endothelial hyperpolarization. As these multiple effects of LPI occur within the same concentration range, it seems very likely that the changes in the properties of the plasma membrane rather than direct action on a specific protein underlie the observed actions. Our results exclude the role of superoxide anions in the inhibitory effect of LPI on NCX, since treatment with the superoxide dismutase mimetic tempol failed to prevent I_{NCX} inhibition.

The inhibition of the hyperpolarization by LPI was not specific to histamine and was reproduced in intact endothelium of excised mice aorta stimulated with Ach. In addition, pre-incubation with LPI results in inhibition of not only the sustained component of hyperpolarization, but effectively suppresses the peak hyperpolarization to Ach. Because the initial transient hyperpolarization to Ach is triggered by stimulation of IK_{Ca} channels following Ca^{2+} release from ER, the inhibition of the transient hyperpolarization by LPI points for engagement of reversed NCX in ER Ca^{2+} refilling in EC. This conclusion was further supported by showing that bepridil suppresses both the sustained and the peak hyperpolarizations of EA.hy926 cells elicited by consecutive histamine applications.

Functional effects of inhibition of NCX in the vasculature are not limited to a suppression of endothelium-dependent relaxation. In smooth muscle cells stimulated with agonists, an increase in the cytosolic Ca^{2+} concentration occurs via NCX-mediated Ca^{2+} entry [50,51].

Accordingly, NCX inhibition or knock-down in smooth muscle cells results in a marked attenuation of vasoconstriction to phenylephrine in mouse mesenteric arteries and drop in blood pressure [52]. Our findings that LPI, LPC16:0 as well as endocannabinoids anandamide and NAGly [38] inhibit NCX may at least partially explain the endothelium-independent component of vasodilation to cannabinoids and lipid-related compounds reported in a variety of vascular beds [53,54]. A failure of LPI to inhibit the hyperpolarization of in situ endothelium to SKA-31 highlights key differences, in terms of NCX involvement, in the mechanisms of the hyperpolarizing responses initiated by Ach, which is frequently used as indirect IK_{Ca}/SK_{Ca} activator, and by SKA-31, a direct IK_{Ca}/SK_{Ca} activator.

Experiments with chelating of intracellular Ca^{2+} with BAPTA-AM in EA.hy926 cells, an approach that favours stimulation of a reversed mode of the exchanger, showed that the resting membrane potential is significantly hyperpolarized as compared to the control cells. We showed that Ca^{2+} removal as well as NCX inhibitors bepridil and KB-R7943 elicit a depolarization. These observations indicate that under conditions of chelating of intracellular Ca^{2+} the exchanger operates in a reversed mode contributing to Ca^{2+} entry. It is still unclear, whether NCX operates in a reverse under control resting conditions. While energetics of the exchanger predicts that at resting membrane potential of -40 mV and intracellular Ca^{2+} level 100 nM, NCX operates in a reverse mode, our early observations indicate that NCX inhibitors benzamil and KB-R7943 have no effect on the resting membrane potential of endothelial cells of excised aorta [37], while strongly inhibit the hyperpolarization to Ach. We show here that under conditions of chelating of cytosolic Ca^{2+} , the histamine response turns to a Na^{+} -dependent depolarization. In Ca^{2+} -free solution, the depolarization appeared to be more sustained than that observed in the presence of bath Ca^{2+} . A possible explanation of this observation is that in the presence of bath Ca^{2+} , Na^{+} entered via histamine-stimulated Na^{+} permeable channels is extruded by the reversed NCX.

In cultured HUVECs, oxidized LDL and, specifically, LPC16:0, were shown to increase the level of intracellular Ca^{2+} due to stimulation of Ca^{2+} entry and, as a consequence, stimulation of BK_{Ca} channels [16]. Here we show that LPC16:0 stimulates BK_{Ca} activity even under fixed Ca^{2+} and voltage, which enabled us to identify LPC16:0 as a direct modulator of BK_{Ca} channels.

In endothelial cells, SOCE regulated by mitochondria has long been considered the primarily Ca^{2+} entry pathway responsible for store refilling [55,56]. This conclusion was based on measurements of Ca^{2+} -sensitive fluorescence during Ca^{2+} re-addition protocol. An increase in fluorescence following Ca^{2+} re-addition after a period of exposure to a Ca^{2+} -free solution, during which agonists or inhibitors of endoplasmic reticulum Ca^{2+} ATPase (SERCA) are applied, is generally interpreted as SOCE [55,56]. In our view, a major weakness in this interpretation is that intracellular Ca^{2+} mobilization in the absence of external Ca^{2+} inevitably results in Ca^{2+} extrusion from the cytosol in exchange for Na^{+} (forward mode of NCX) and, consequently, in accumulation of cytosolic Na^{+} accompanied by membrane depolarization. As NCX is a voltage-dependent transporter, cell depolarization would facilitate the reversed NCX as soon as Ca^{2+} is added to the bath. By utilizing NCX blockers bepridil and KB-R7943 we show that both compounds strongly suppress the

hyperpolarizing responses induced by Ca^{2+} -re-introduction. These findings, together with the ability of histamine to stimulate the outwardly rectifying current with negative reversal potential, a typical characteristic of NCX, but not the inwardly rectifying current with positive reversal potential characteristic of SOCE [57], strongly indicate for NCX involvement in Ca^{2+} entry in the cells studied. In addition, we found that bepridil and KB-R7943 largely suppress peak hyperpolarization to consecutive administrations of Ach and histamine, delineating NCX involvement in ER Ca^{2+} refilling in EC.

5 Conclusions

In summary, we showed that LPC16:0 has a direct modulatory action on BK_{Ca} activity which results in EC hyperpolarization. In addition, LPC16:0 and LPI inhibit EC hyperpolarization to histamine and Ach via suppression of Ca^{2+} entry driven by NCX required for ER refilling. NCX inhibition is non-mode-specific, independent of GPCR and superoxide anions and is observed both in vitro and in situ EC. Our results further emphasize a crucial role of NCX in Ca^{2+} entry and ER Ca^{2+} refilling in EC, challenging the concept of mitochondria-regulated SOCE as a unique primary Ca^{2+} influx pathway in the endothelium. This newly identified mechanism of action of LPI and LPC may underlie a suppression of endothelium-dependent relaxation and endothelial dysfunction under pathological conditions accompanied by increased levels of these LPL in the blood and atherosclerotic arterial lesions.

Funding

This study was supported by grants from Swiss National Science Foundation (SNSF, #310030_152639/1 and #IZ73Z0_152578) and Austrian Science Fund (FWF, P27238-B27). The Institute of Physiology NAS of Ukraine is grateful for electrophysiological equipment purchased with SNSF grant #IZ73Z0_152578.

References

- [1]. Drzazga A, Sowinska A, Koziolkiewicz M. Lysophosphatidylcholine and lysophosphatidylinositol—novel promising signaling molecules and their possible therapeutic activity. *Acta Pol Pharm.* 2014; 71(6):887–899. [PubMed: 25745761]
- [2]. Ouweneel AB, Van Eck M. Lipoproteins as modulators of atherothrombosis: from endothelial function to primary and secondary coagulation. *Vasc Pharmacol.* 2016; 82:1–10.
- [3]. Colic M, Pantovic S, Jeremic M, Jokovic V, Obradovic Z, Rosic M. Transport of low-density lipoprotein into the blood vessel wall during atherogenic diet in the isolated rabbit carotid artery. *Circ J.* 2015; 79(8):1846–1852. [PubMed: 25993902]
- [4]. Vanhoutte PM. Endothelial dysfunction: the first step toward coronary arteriosclerosis. *Circ J.* 2009; 73(4):595–601. [PubMed: 19225203]
- [5]. Shimokawa H. Primary endothelial dysfunction: atherosclerosis. *J Mol Cell Cardiol.* 1999; 31(1): 23–37. [PubMed: 10072713]
- [6]. Kruzliak P, Sabo J, Zulli A. Endothelial endoplasmic reticulum and nitrate stress in endothelial dysfunction in the atherogenic rabbit model. *Acta Histochem.* 2015; 117(8):762–766. [PubMed: 26359324]
- [7]. Sonoki K, Iwase M, Iino K, Ichikawa K, Ohdo S, Higuchi S, Yoshinari M, Iida M. Atherogenic role of lysophosphatidylcholine in low-density lipoprotein modified by phospholipase A2 and in diabetic patients: protection by nitric oxide donor. *Metabolism.* 2003; 52(3):308–314. [PubMed: 12647268]
- [8]. Kohno M, Yokokawa K, Yasunari K, Minami M, Kano H, Hanehira T, Yoshikawa J. Induction by lysophosphatidylcholine, a major phospholipid component of atherogenic lipoproteins, of human

- coronary artery smooth muscle cell migration. *Circulation*. 1998; 98(4):353–359. [PubMed: 9711941]
- [9]. Menon NK, Saito T, Wolf A, Bing RJ. Correlation of lysophosphatidylcholine-induced vs spontaneous relaxation to cyclic GMP levels in rabbit thoracic aorta. *Life Sci*. 1989; 44(9):611–618. [PubMed: 2538701]
- [10]. Dudek R, Conforto A, Bing RJ. Lysophosphatidylcholine-induced vascular relaxation and production of cGMP are mediated by endothelium-derived relaxing factor. *Proc Soc Exp Biol Med*. 1993; 203(4):474–479. [PubMed: 8394588]
- [11]. Hirayama T, Ogawa Y, Tobise K, Kikuchi K. Mechanism of endothelium-dependent vasorelaxation evoked by lysophosphatidylcholine. *Hypertens Res*. 1998; 21(3):137–145. [PubMed: 9786596]
- [12]. Yokoyama K, Ishibashi T, Ohkawara H, Kimura J, Matsuoka I, Sakamoto T, Nagata K, Sugimoto K, Sakurada S, Maruyama Y. HMG-CoA reductase inhibitors suppress intracellular calcium mobilization and membrane current induced by lysophosphatidylcholine in endothelial cells. *Circulation*. 2002; 105(8):962–967. [PubMed: 11864926]
- [13]. Su Z, Ling Q, Guo ZG. Effects of lysophosphatidylcholine on bovine aortic endothelial cells in culture. *Cardioscience*. 1995; 6(1):31–37. [PubMed: 7605894]
- [14]. Kim MY, Liang GH, Kim JA, Choi SS, Choi S, Suh SH. Oxidized low-density lipoprotein- and lysophosphatidylcholine-induced Ca mobilization in human endothelial cells. *Korean J Physiol Pharmacol*. 2009; 13(1):27–32. [PubMed: 19885023]
- [15]. Wong JT, Tran K, Pierce GN, Chan AC, O K, Choy PC. Lysophosphatidylcholine stimulates the release of arachidonic acid in human endothelial cells. *J Biol Chem*. 1998; 273(12):6830–6836. [PubMed: 9506985]
- [16]. Kuhlmann WCR, Wiebke Ludders D, Schaefer CA, Kerstin Most A, Backenkohler U, Neumann T, Tillmanns H, Erdogan A. Lysophosphatidylcholine-induced modulation of Ca(2+)-activated K(+)channels contributes to ROS-dependent proliferation of cultured human endothelial cells. *J Mol Cell Cardiol*. 2004; 36(5):675–682. [PubMed: 15135662]
- [17]. Miwa Y, Hirata K, Kawashima S, Akita H, Yokoyama M. Lysophosphatidylcholine inhibits receptor-mediated Ca²⁺ mobilization in intact endothelial cells of rabbit aorta. *Arterioscler Thromb Vasc Biol*. 1997; 17(8):1561–1567. [PubMed: 9301636]
- [18]. Cowan CL, Steffen RP. Lysophosphatidylcholine inhibits relaxation of rabbit abdominal aorta mediated by endothelium-derived nitric oxide and endothelium-derived hyperpolarizing factor independent of protein kinase C activation. *Arterioscler Thromb Vasc Biol*. 1995; 15(12):2290–2297. [PubMed: 7489255]
- [19]. Huang TY, Chen HI, Liu CY, Jen CJ. Lysophosphatidylcholine alters vascular tone in rat aorta by suppressing endothelial [Ca²⁺]_i signaling. *J Biomed Sci*. 2002; 9(4):327–333. [PubMed: 12145530]
- [20]. Zhang R, Rodrigues B, MacLeod KM. Lysophosphatidylcholine potentiates phenylephrine responses in rat mesenteric arterial bed through modulation of thromboxane A₂. *J Pharmacol Exp Ther*. 2006; 317(1):355–361. [PubMed: 16394197]
- [21]. Eizawa H, Yui Y, Inoue R, Kosuga K, Hattori R, Aoyama T, Sasayama S. Lysophosphatidylcholine inhibits endothelium-dependent hyperpolarization and N omega-nitro-L-arginine/indomethacin-resistant endothelium-dependent relaxation in the porcine coronary artery. *Circulation*. 1995; 92(12):3520–3526. [PubMed: 8521575]
- [22]. Safaya R, Chai H, Kougiaris P, Lin P, Lumsden A, Yao Q, Chen C. Effect of lysophosphatidylcholine on vasomotor functions of porcine coronary arteries. *J Surg Res*. 2005; 126(2):182–188. [PubMed: 15919417]
- [23]. Fukao M, Hattori Y, Kanno M, Sakuma I, Kitabatake A. Structural differences in the ability of lysophospholipids to inhibit endothelium-dependent hyperpolarization by acetylcholine in rat mesenteric arteries. *Biochem Biophys Res Commun*. 1996; 227(2):479–483. [PubMed: 8878540]
- [24]. Rao SP, Riederer M, Lechleitner M, Hermansson M, Desoye G, Hallstrom S, Graier WF, Frank S. Acyl chain-dependent effect of lysophosphatidylcholine on endothelium-dependent vasorelaxation. *PLoS One*. 2013; 8(5):e65155. [PubMed: 23741477]

- [25]. Choi S, Park S, Liang GH, Kim JA, Suh SH. Superoxide generated by lysophosphatidylcholine induces endothelial nitric oxide synthase downregulation in human endothelial cells. *Cell Physiol Biochem*. 2010; 25(2–3):233–240. [PubMed: 20110684]
- [26]. Froese DE, McMaster J, Man RY, Choy PC, Kroeger EA. Inhibition of endothelium-dependent vascular relaxation by lysophosphatidylcholine: impact of lysophosphatidylcholine on mechanisms involving endothelium-derived nitric oxide and endothelium derived hyperpolarizing factor. *Mol Cell Biochem*. 1999; 197(1–2):1–6. [PubMed: 10485317]
- [27]. Fukao M, Hattori Y, Kanno M, Sakuma I, Kitabatake A. Evidence for selective inhibition by lysophosphatidylcholine of acetylcholine-induced endothelium-dependent hyperpolarization and relaxation in rat mesenteric artery. *Br J Pharmacol*. 1995; 116(1):1541–1543. [PubMed: 8564216]
- [28]. Min Z, Kang L, Lin L, Jinghua F, Junna S, Baolin L. Resveratrol restores lysophosphatidylcholine-induced loss of endothelium-dependent relaxation in rat aorta tissue coinciding with inhibition of extracellular-signal-regulated protein kinase activation. *Phytother Res*. 2010; 24(12):1762–1768. [PubMed: 20564508]
- [29]. Oka S, Nakajima K, Yamashita A, Kishimoto S, Sugiura T. Identification of GPR55 as a lysophosphatidylinositol receptor. *Biochem Biophys Res Commun*. 2007; 362(4):928–934. [PubMed: 17765871]
- [30]. AlSuleimani YM, Hiley CR. The GPR55 agonist lysophosphatidylinositol relaxes rat mesenteric resistance artery and induces Ca^{2+} release in rat mesenteric artery endothelial cells. *Br J Pharmacol*. 2015; 172(12):3043–3057. [PubMed: 25652040]
- [31]. Bondarenko A, Waldeck-Weiermair M, Naghdi S, Poteser M, Malli R, Graier WF. GPR55-dependent and -independent ion signalling in response to lysophosphatidylinositol in endothelial cells. *Br J Pharmacol*. 2010; 161(2):308–320. [PubMed: 20735417]
- [32]. Bondarenko A, Panasiuk O, Stepanenko L, Goswami N, Sagach V. Reduced hyperpolarization of endothelial cells following high dietary Na^+ : effects of enalapril and tempol. *Clin Exp Pharmacol Physiol*. 2012; 39(7):608–613. [PubMed: 22540516]
- [33]. Kohler R, Ruth P. Endothelial dysfunction and blood pressure alterations in K^+ -channel transgenic mice. *Pflugers Arch*. 2010; 459(6):969–976. [PubMed: 20349244]
- [34]. Nilius B, Droogmans G. Ion channels and their functional role in vascular endothelium. *Physiol Rev*. 2001; 81(4):1415–1459. [PubMed: 11581493]
- [35]. Wang X, Reznick S, Li P, Liang W, van Breemen C. Ca^{2+} removal mechanisms in freshly isolated rabbit aortic endothelial cells. *Cell Calcium*. 2002; 31(6):265–277. [PubMed: 12098216]
- [36]. Graier WF, Paltauf-Doburzynska J, Hill BJ, Fleischhacker E, Hoebel BG, Kostner GM, Sturek M. Submaximal stimulation of porcine endothelial cells causes focal Ca^{2+} elevation beneath the cell membrane. *J Physiol*. 1998; 506(Pt 1):109–125. [PubMed: 9481676]
- [37]. Bondarenko A. Sodium-calcium exchanger contributes to membrane hyperpolarization of intact endothelial cells from rat aorta during acetylcholine stimulation. *Br J Pharmacol*. 2004; 143(1):9–18. [PubMed: 15289290]
- [38]. Bondarenko AI, Drachuk K, Panasiuk O, Sagach V, Deak AT, Malli R, Graier WF. N-arachidonoyl glycine suppresses $\text{Na}^+/\text{Ca}^{2+}$ exchanger-mediated Ca^{2+} entry into endothelial cells and activates BK channels independently of G-protein coupled receptors. *Br J Pharmacol*. 2013; 169(4):933–948. [PubMed: 23517055]
- [39]. Girardin NC, Antigny F, Frieden M. Electrophysiological characterization of storeoperated and agonist-induced Ca^{2+} entry pathways in endothelial cells. *Pflugers Arch*. 2010; 460(1):109–120. [PubMed: 20419508]
- [40]. Andrikopoulos P, Baba A, Matsuda T, Djamgoz MB, Yaqoob MM, Eccles SA. Ca^{2+} influx through reverse mode $\text{Na}^+/\text{Ca}^{2+}$ exchange is critical for vascular endothelial growth factor-mediated extracellular signal-regulated kinase (ERK) 1/2 activation and angiogenic functions of human endothelial cells. *J Biol Chem*. 2011; 286(44):37919–37931. [PubMed: 21873429]
- [41]. Edgell CJ, McDonald CC, Graham JB. Permanent cell line expressing human factor VIII-related antigen established by hybridization. *Proc Natl Acad Sci U S A*. 1983; 80(12):3734–3737. [PubMed: 6407019]

- [42]. Watanabe Y, Kimura J. Blocking effect of bepridil on $\text{Na}^+/\text{Ca}^{2+}$ exchange current in guinea pig cardiac ventricular myocytes. *Jpn J Pharmacol.* 2001; 85(4):370–375. [PubMed: 11388640]
- [43]. Bondarenko AI, Malli R, Graier WF. The GPR55 agonist lysophosphatidylinositol directly activates intermediate-conductance Ca^{2+} -activated K^+ channels. *Pflugers Arch.* 2011; 462(2): 245–255. [PubMed: 21603896]
- [44]. Marchenko SM, Sage SO. Electrical properties of resting and acetylcholine-stimulated endothelium in intact rat aorta. *J Physiol.* 1993; 462:735–751. [PubMed: 8331598]
- [45]. Bondarenko AI, Malli R, Graier WF. The GPR55 agonist lysophosphatidylinositol acts as an intracellular messenger and bidirectionally modulates Ca^{2+} -activated large-conductance K^+ channels in endothelial cells. *Pflugers Arch.* 2011; 461(1):177–189. [PubMed: 21072666]
- [46]. d'Uscio LV, Smith LA, Katusic ZS. Hypercholesterolemia impairs endothelium-dependent relaxations in common carotid arteries of apolipoprotein e-deficient mice. *Stroke.* 2001; 32(11): 2658–2664. [PubMed: 11692031]
- [47]. Matsumoto T, Kobayashi T, Kamata K. Role of lysophosphatidylcholine (LPC) in atherosclerosis. *Curr Med Chem.* 2007; 14(30):3209–3220. [PubMed: 18220755]
- [48]. Zhang Y, Zhang W, Edvinsson L, Xu CB. Apolipoprotein B of low-density lipoprotein impairs nitric oxide-mediated endothelium-dependent relaxation in rat mesenteric arteries. *Eur J Pharmacol.* 2014; 725:10–17. [PubMed: 24444440]
- [49]. Bondarenko A, Sagach V. Na^+/K^+ -ATPase is involved in the sustained ACh-induced hyperpolarization of endothelial cells from rat aorta. *Br J Pharmacol.* 2006; 149(7):958–965. [PubMed: 17001300]
- [50]. Zhao J, Majewski H. Endothelial nitric oxide attenuates $\text{Na}^+/\text{Ca}^{2+}$ exchanger-mediated vasoconstriction in rat aorta. *Br J Pharmacol.* 2008; 154(5):982–990. [PubMed: 18469841]
- [51]. Nishimura J. Topics on the $\text{Na}^+/\text{Ca}^{2+}$ exchanger: involvement of $\text{Na}^+/\text{Ca}^{2+}$ exchanger in the vasodilator-induced vasorelaxation. *J Pharmacol Sci.* 2006; 102(1):27–31. [PubMed: 16990700]
- [52]. Zhang J, Ren C, Chen L, Navedo MF, Antos LK, Kinsey SP, Iwamoto T, Philipson KD, Kotlikoff MI, Santana LF, Wier WG, et al. Blaustein, Knockout of $\text{Na}^+/\text{Ca}^{2+}$ exchanger in smooth muscle attenuates vasoconstriction and L-type Ca^{2+} channel current and lowers blood pressure. *Am J Physiol Heart Circ Physiol.* 2010; 298(5):H1472–H1483. [PubMed: 20173044]
- [53]. Bondarenko AI. Endothelial atypical cannabinoid receptor: do we have enough evidence? *Br J Pharmacol.* 2014; 171(24):5573–5588. [PubMed: 25073723]
- [54]. Al Suleimani YM, Al Mahruqi AS, Hiley CR. Mechanisms of vasorelaxation induced by the cannabidiol analogue compound O-1602 in the rat small mesenteric artery. *Eur J Pharmacol.* 2015; 765:107–114. [PubMed: 26297305]
- [55]. Malli R, Frieden M, Osibow K, Zoratti C, Mayer M, Demareux N, Graier WF. Sustained Ca^{2+} transfer across mitochondria is essential for mitochondrial Ca^{2+} buffering, store-operated Ca^{2+} entry, and Ca^{2+} store refilling. *J Biol Chem.* 2003; 278(45):44769–44779. [PubMed: 12941956]
- [56]. Naghdi S, Waldeck-Weiermair M, Fertschai I, Poteser M, Graier WF, Malli R. Mitochondrial Ca^{2+} uptake and not mitochondrial motility is required for STIM1-Orai1-dependent store-operated Ca^{2+} entry. *J Cell Sci.* 2010; 123(Pt 15):2553–2564. [PubMed: 20587595]
- [57]. Fasolato C, Nilius B. Store depletion triggers the calcium release-activated calcium current (ICRAC) in macrovascular endothelial cells: a comparison with Jurkat and embryonic kidney cell lines. *Pflugers Arch.* 1998; 436(1):69–74. [PubMed: 9560448]

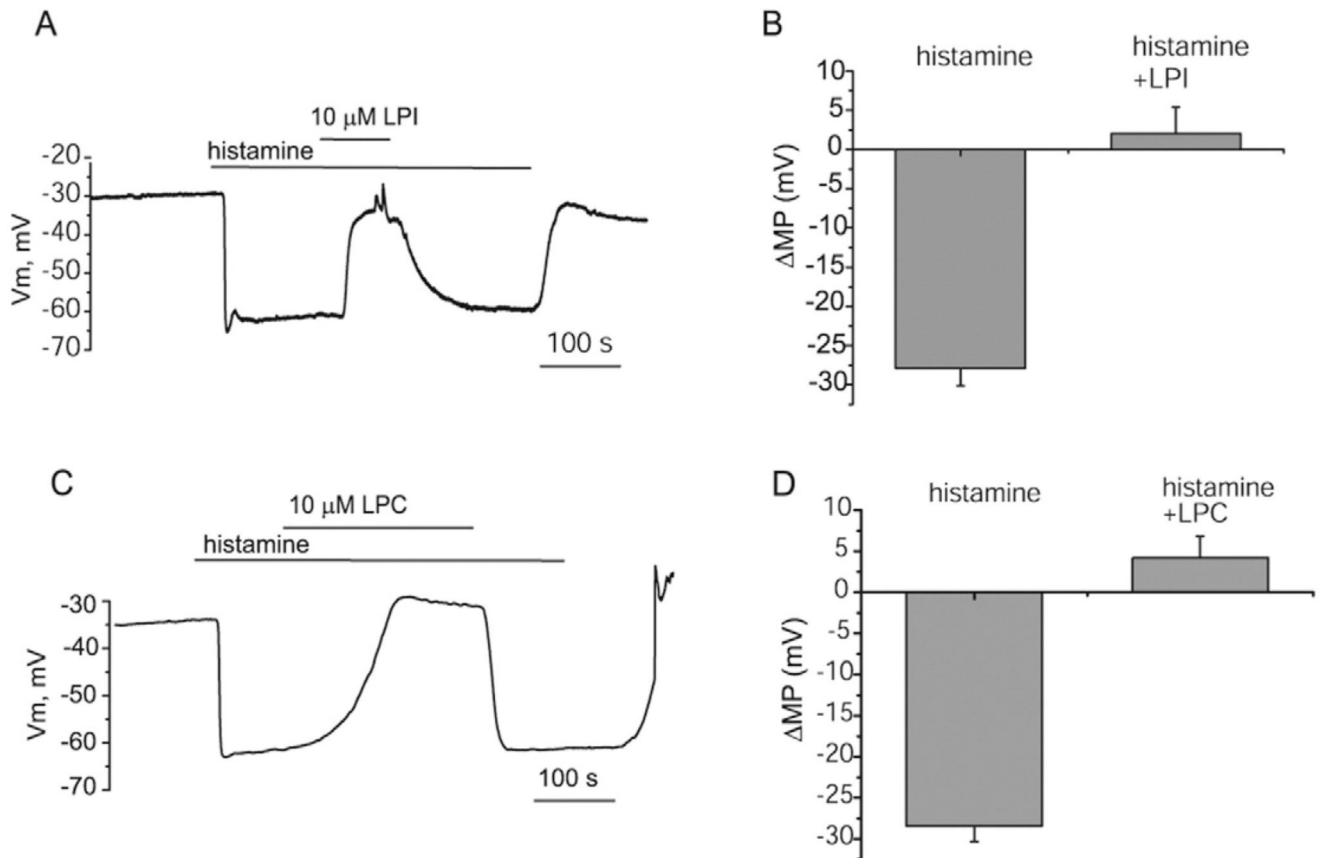


Fig. 1. LPI and LPC16:0 suppress hyperpolarization of EA.hy926 cells to histamine.

(A) Membrane potential recording showing inhibition of the sustained hyperpolarization to 100 μ M histamine by 10 μ M LPC16:0, (B) Statistical representation showing the amplitude of membrane potential responses to histamine before and after addition of 10 μ M LPC16:0. (C) Membrane potential recording showing the effect of LPI on the hyperpolarization elicited by 100 μ M histamine, (D) Bars show mean values of the amplitude of membrane potential deflections to histamine before and after addition of 10 μ M LPI.

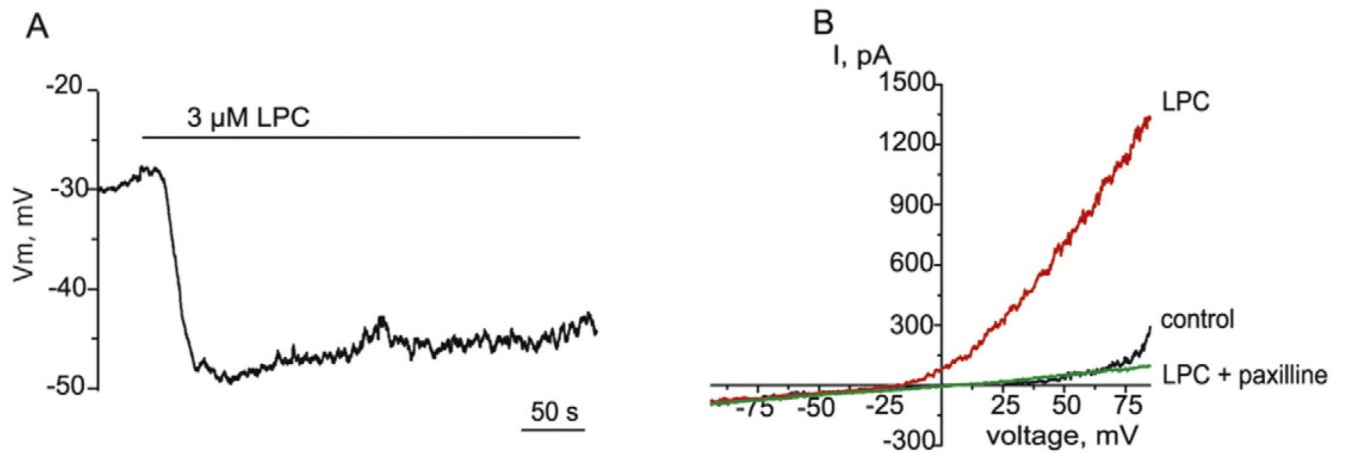


Fig. 2. LPC16:0 produces hyperpolarization of EA.hy926 cells and activation of BK_{Ca} channels independently G-protein coupled receptors.

(A) Membrane potential recording showing the effect of 3 μM LPC16:0 on the membrane potential of EA.hy926 cells. (B) Representative whole-cell K⁺ currents in response to voltage ramps from -80 to +80 mV in the absence (control), and presence of 3 μM LPC16:0 and in the combined presence of 3 μM LPC16:0 and 1 μM paxilline. Exemplary record out of 5 individual experiments.

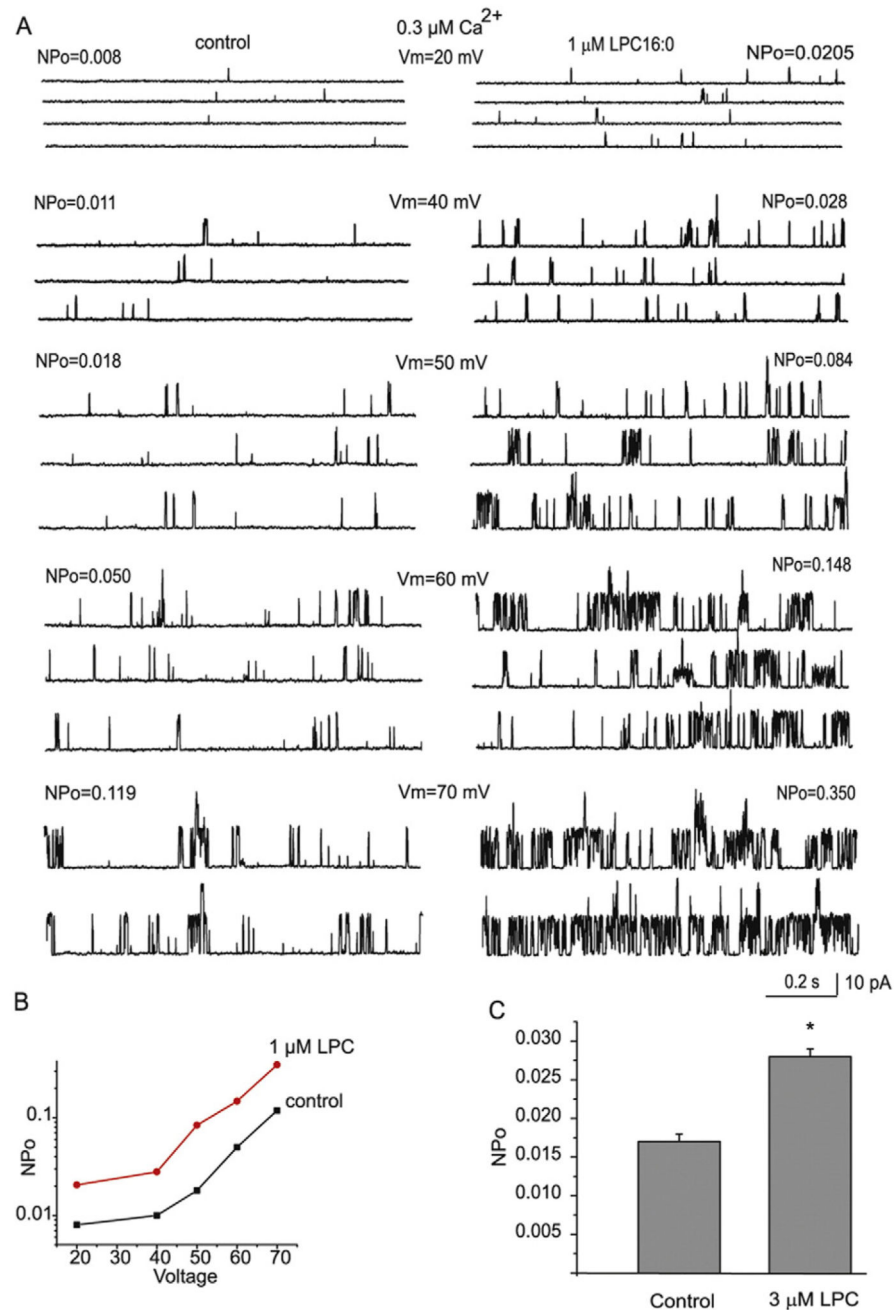


Fig. 3. LPC16:0 stimulates BK_{Ca} single activity independently of GPCR.

(A) Single channel recordings of BK_{Ca} activity in inside-out patches at different voltages indicated and a fixed Ca²⁺ 300 nM before (left) and after (right) administration of 1 μM LPC16:0. (B) Graphical representation of corresponding NPo values under different voltages under control conditions (control) and after administration of 1 μM LPC16:0. (C) Mean NPo values of BK_{Ca} activity in inside-out patches under holding voltage 40 mV and fixed Ca²⁺ 300 nM before and after addition of 3 μM LPC16:0 (n = 9) to the bath.

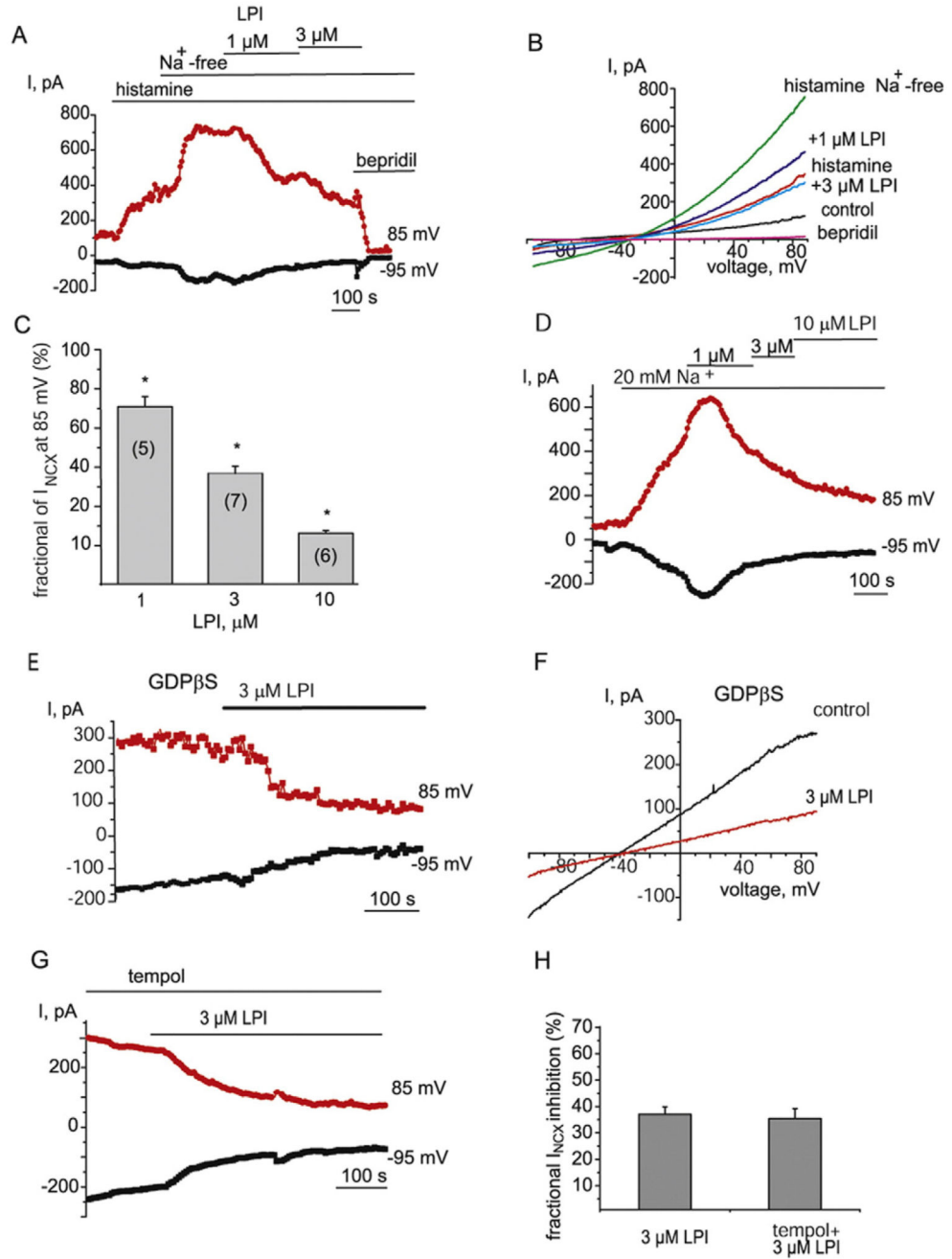


Fig. 4. LPI inhibits both forward and reversed modes of NCX currents independently of GPCR and superoxide anions.

(A) The time course of inhibition of NCX current by 1 and 3 μ M LPI. NCX currents were pre-stimulated with histamine (100 μ M) and substitution of bath Na^+ for NMDG. NCX inhibitor bepridil (100 μ M) was administered at the end of recording. (B) Corresponding NCX currents evoked by voltage ramps from the time course shown in (A) before (control), in the presence of histamine (histamine) and following Na^+ substitution for NMDG before (histamine Na^+ -free) and after administration of 1 μ M LPI (+1 μ M LPI), 3 μ M LPI (+3 μ M LPI) and bepridil (100 μ M). (C) Graphical representation of concentration-dependent effect

of LPI on NCX current amplitude taken at +85 mV. (D) Time course of the effect of 1, 3 and 10 μM LPI on the amplitude of NCX currents pre-stimulated by reduction of bath Na^+ concentration to 20 mM at voltages indicated without prior exposure to histamine ($n = 5$). (E) Time course of the effect of 3 μM LPI on the amplitude of NCX currents taken at -95 mV (forward mode) and 85 mV (reversed mode) in the presence of intracellular $\text{GDP}\beta\text{S}$ (0.5 mM). (F) Corresponding NCX currents evoked by voltage ramps from the time course shown in (E). (G) Representative time course of NCX current before and after addition of 3 μM LPI in the presence of 10 μM tempol ($n = 4$). (H) Bars indicate the mean inhibition of I_{NCX} amplitude by 3 μM LPI in the absence ($n = 7$) and presence ($n = 4$) of tempol (10 μM). Current amplitudes were calculated at 85 mV.

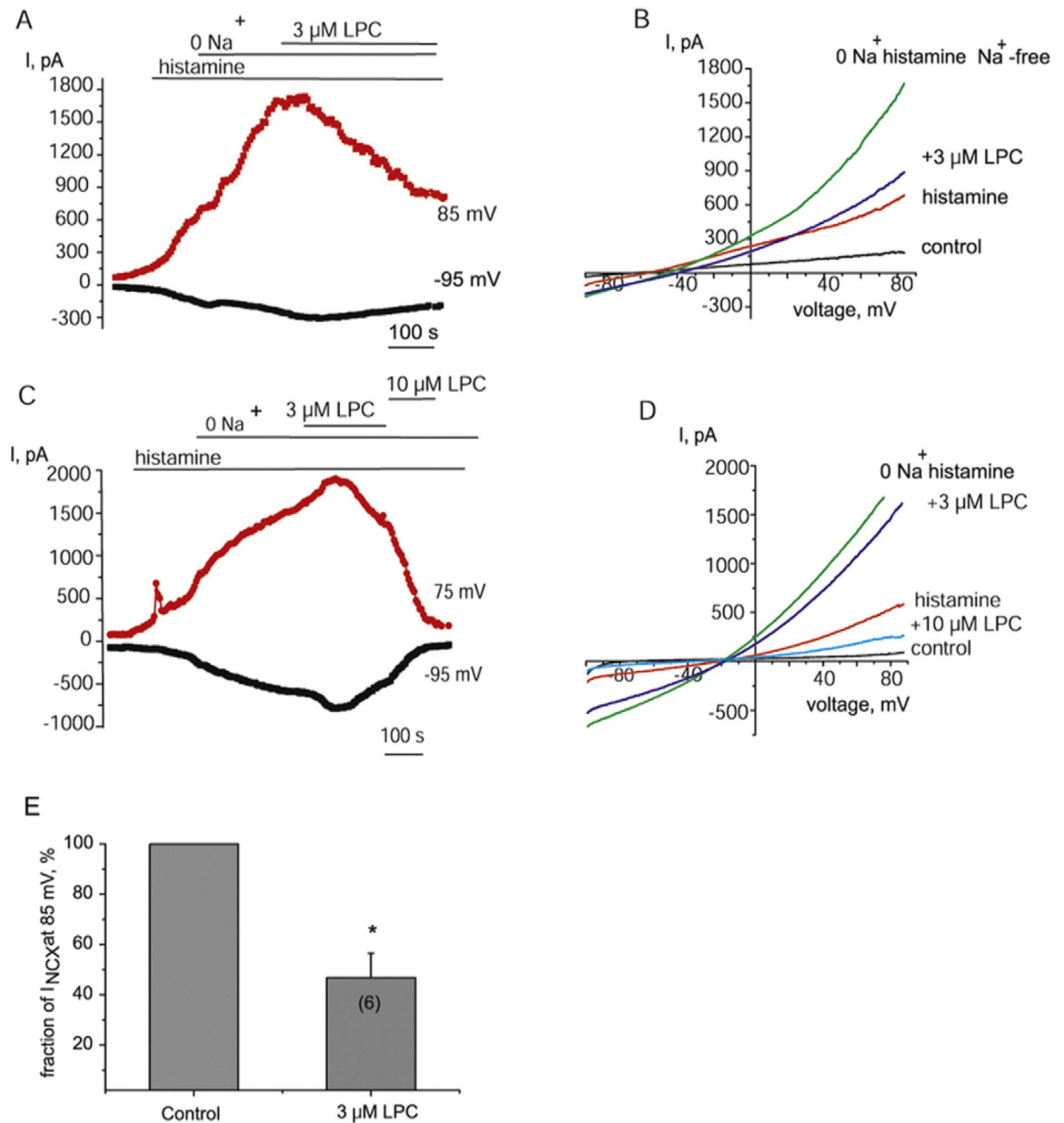


Fig. 5. LPC16:0 inhibits NCX currents.

(A) Representative ($n = 6$) time course of NCX current amplitudes pre-stimulated with histamine and subsequent switch to a Na⁺-free solution followed by administration of 3 μM LPC16:0 during voltage ramps at voltages indicated. (B) Corresponding NCX currents evoked by voltage ramps from the time course shown in (A) under control conditions (control), in the presence of 100 μM histamine (histamine) and following Na⁺ substitution before (histamine Na⁺-free) and after administration of 3 μM LPC16:0. (C) Representative time course of NCX current amplitudes showing accelerated NCX current inhibition by 10

μM LPC16:0. (D) Corresponding current traces in response to voltage ramps from the time course shown in (C). (E) Statistical representation of the inhibitory effect of 3 μM LPC16:0 on NCX current amplitude taken at 85 mV during voltage ramps. The number in brackets indicates the number of cell included in the analysis.

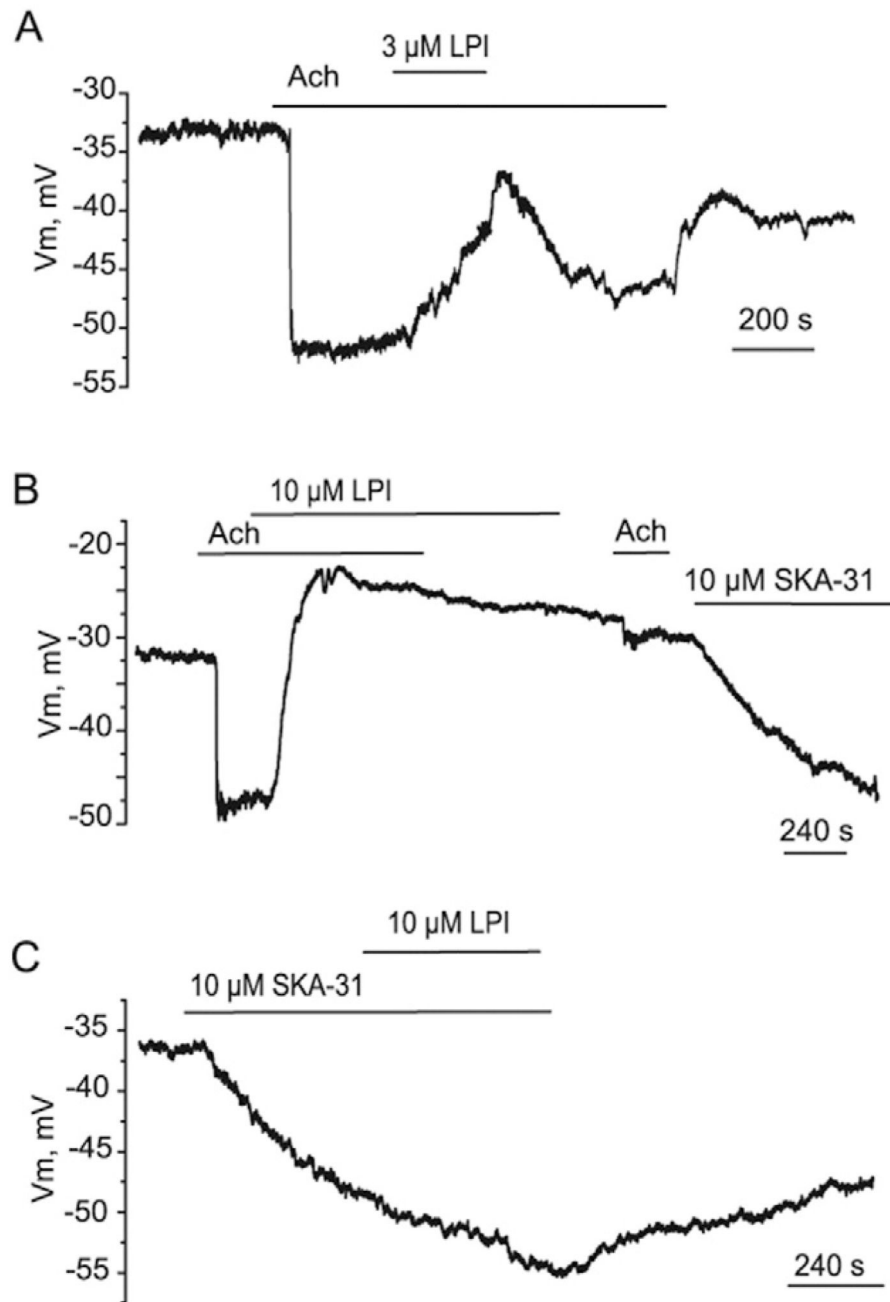


Fig. 6. LPI suppresses the hyperpolarization to Ach, but not to SKA-31, in the endothelium of mice aorta.

(A) Effect of 3 μM LPI on endothelial hyperpolarization to 2 μM Ach ($n = 4$). (B) Effect of 10 μM LPI on endothelial hyperpolarization to two consecutive administrations of 2 μM Ach ($n = 3$). The hyperpolarization to SKA-31 (10 μM) remained unaffected by LPI pre-exposure ($n = 4$). (C) Representative membrane potential recording from in situ mice aortic endothelium showing a failure of LPI (10 μM) to inhibit the hyperpolarization evoked by 10 μM SKA-31 ($n = 3$).

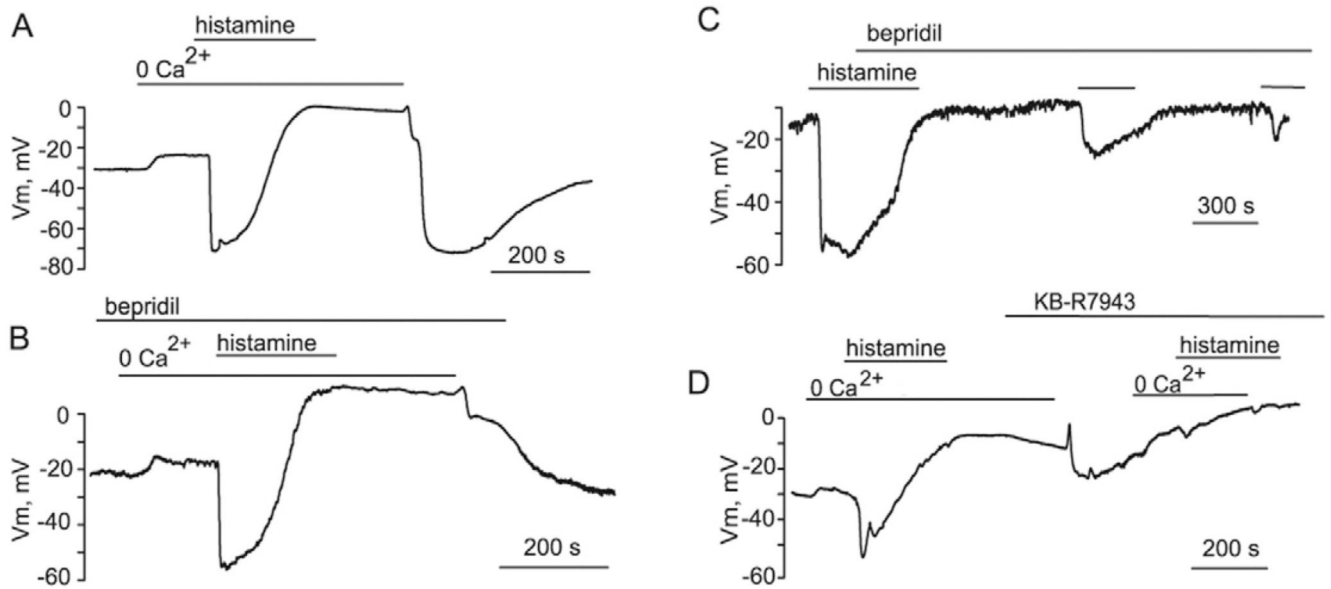


Fig. 7. Reversed NCX is involved in ER Ca²⁺ store refilling in EC.

(A) Typical changes in membrane potential of EA.hy926 cells during Ca²⁺-re-addition protocol. (B) Bepridil (20 μM) inhibits the hyperpolarization induced by Ca²⁺ re-addition (n = 4). (C) Bepridil inhibits both the transient and sustained components of hyperpolarization induced by consecutive administrations of 100 μM histamine (n = 4). (D) Effect of KB-R7943 (20 μM) on the hyperpolarization induced by Ca²⁺ re-addition and subsequent exposure to 100 μM histamine (n = 3).

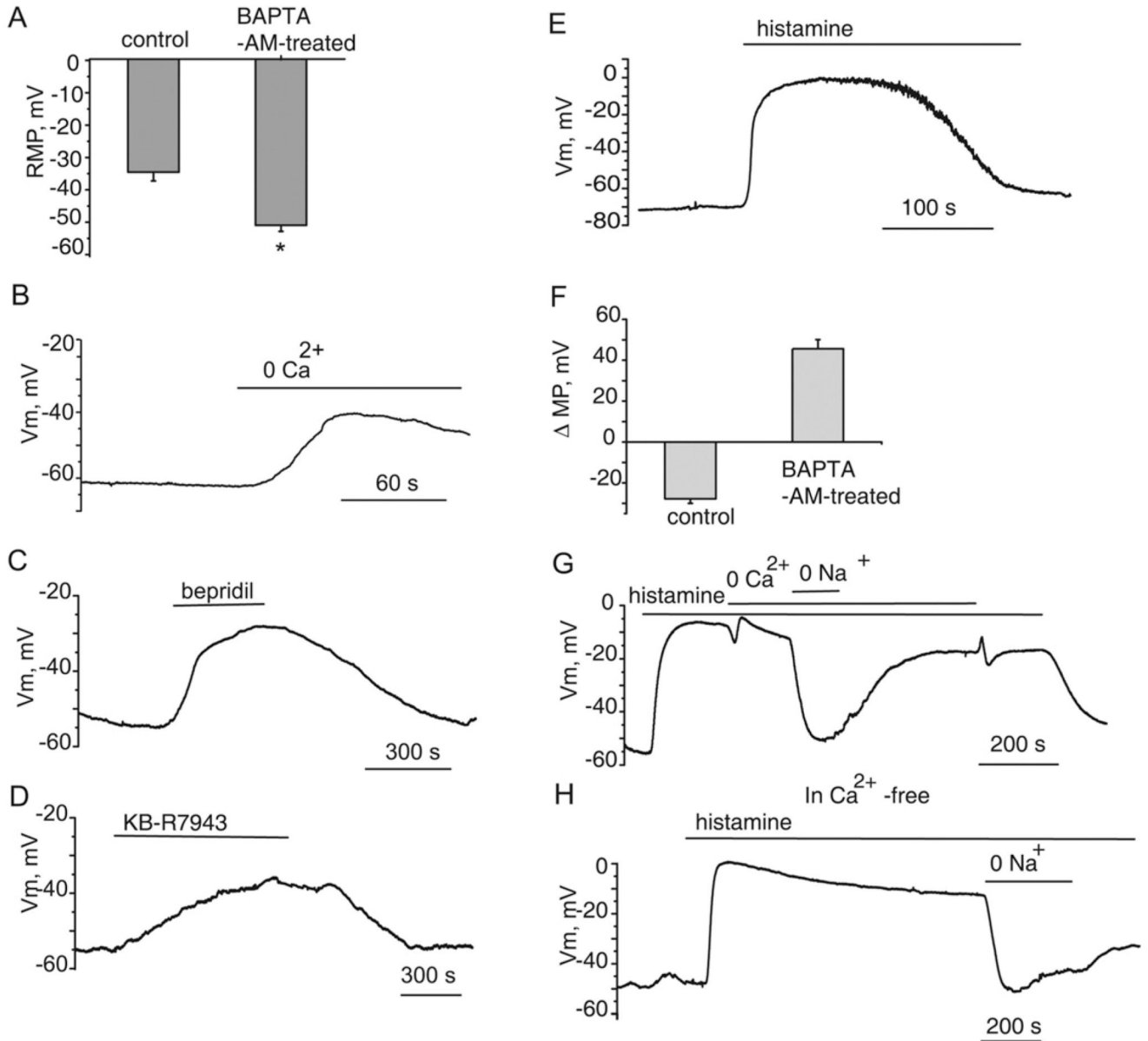


Fig. 8. Buffering of intracellular Ca^{2+} uncovers Na^+ -dependent membrane depolarization of EA.hy926 cells in response to histamine.

(A) Bars showing the mean membrane potential values of unstimulated EA.hy926 cells under control conditions ($n = 11$) and following cytosolic Ca^{2+} buffering with BAPTA-AM ($n = 13$). (B) The membrane potential record showing the effect of superfusion with Ca^{2+} -free solution containing 1 mM EGTA following pre-incubation with 20 μM BAPTA-AM. (C) The membrane potential record showing the effect of 100 μM bepridil on the resting membrane potential following chelation of cytosolic Ca^{2+} with 20 μM BAPTA-AM. (D) The effect of 20 μM KB-R7943 on the membrane potential following chelation of cytosolic Ca^{2+} . (E) The membrane potential record showing the effect of 100 histamine on the membrane potential following chelation of cytosolic Ca^{2+} with 20 μM BAPTA-AM. (F)

Bars showing average shifts in the membrane potential of EA.hy926 endothelial cells induced by 100 μM histamine under control conditions and following chelation of cytosolic Ca^{2+} with 20 μM BAPTA-AM. (G) Exemplary membrane potential record showing the effect of Ca^{2+} and Na^{+} removal on the histamine-induced depolarization of EA.hy926 cells pre-incubated with BAPTA-AM. (H) Membrane potential record showing the effect of histamine applied in a Ca^{2+} free solution shortly after Ca^{2+} removal. Cells were pre-incubated with BAPTA-AM. Note a sustained Na^{+} -dependent depolarization with a long decay as compared with that observed in a Ca^{2+} -containing solution (panel E).